A&A 365, 491–507 (2001)
DOI: 10.1051/0004-6361:20000147

Astronomy & Astrophysics

Population synthesis for double white dwarfs

I. Close detached systems

G. Nelemans[1], L. R. Yungelson[1,2], S. F. Portegies Zwart[3,⋆], and F. Verbunt[4]

[1] Astronomical Institute "Anton Pannekoek", Kruislaan 403, 1098 SJ Amsterdam, The Netherlands
e-mail: gijsn@astro.uva.nl
[2] Institute of Astronomy of the Russian Academy of Sciences, 48 Pyatnitskaya Str., 109017 Moscow, Russia
e-mail: lry@inasan.rssi.ru
[3] Department of Physics and Center for Space Research, MIT, 77 Massachusetts Avenue, Cambridge, MA 02139, USA
e-mail: spz@space.mit.edu
[4] Astronomical Institute, Utrecht University, PO Box 80000, 3508 TA Utrecht, The Netherlands
e-mail: F.W.M.Verbunt@astro.uu.nl

Received 3 July 2000 / Accepted 19 October 2000

Abstract. We model the population of double white dwarfs in the Galaxy and find a better agreement with observations compared to earlier studies, due to two modifications. The first is the treatment of the first phase of unstable mass transfer and the second the modelling of the cooling of the white dwarfs. A satisfactory agreement with observations of the local sample of white dwarfs is achieved if we assume that the initial binary fraction is ∼50% and that the lowest mass white dwarfs ($M < 0.3\,M_\odot$) cool faster than the most recently published cooling models predict. With this model we find a Galactic birth rate of close double white dwarfs of 0.05 yr^{-1}, a birth rate of AM CVn systems of 0.005 yr^{-1}, a merger rate of pairs with a combined mass exceeding the Chandrasekhar limit (which may be progenitors of SNe Ia) of 0.003 yr^{-1} and a formation rate of planetary nebulae of 1 yr^{-1}. We estimate the total number of double white dwarfs in the Galaxy as 2.5 10^8. In an observable sample with a limiting magnitude $V_{\rm lim} = 15$ we predict the presence of ∼855 white dwarfs of which ∼220 are close pairs. Of these 10 are double CO white dwarfs of which one has a combined mass exceeding the Chandrasekhar limit and will merge within a Hubble time.

Key words. stars: white dwarfs – stars: statistics – binaries: close – binaries: evolution

1. Introduction

Close double white dwarfs[1] form an interesting population for a number of reasons. First they are binaries that have experienced at least two phases of mass transfer and thus provide good tests for theories of binary evolution. Second it has been argued that type Ia supernovae arise from merging double CO white dwarfs (Webbink 1984; Iben & Tutukov 1984). Thirdly close double white dwarfs may be the most important contributors to the gravitational wave signal at low frequencies, probably even producing an unresolved noise burying many underlying signals (Evans et al. 1987; Hils et al. 1990). A fourth reason to study the population of double white dwarfs is that in combination with binary evolution theories, the recently developed detailed cooling models for (low-mass) white dwarfs can be tested.

The formation of the population of double white dwarfs has been studied analytically by Iben & Tutukov (1986a, 1987) and numerically by Lipunov & Postnov (1988); Tutukov & Yungelson (1993, 1994); Yungelson et al. (1994); Han et al. (1995); Iben et al. (1997, hereafter ITY97), and Han (1998, hereafter HAN98). Comparison between these studies gives insight in the differences that exist between the assumptions made in different synthesis calculations.

Following the discovery of the first close double white dwarf (Saffer et al. 1988), the observed sample of such systems in which the mass of at least one component is measured has increased to 14 (Maxted & Marsh 1999; Maxted et al. 2000). This makes it possible to compare the models to the observations in more detail.

Send offprint requests to: G. Nelemans
⋆ Hubble Fellow.
[1] Throughout this work we'll use the term double white dwarf instead of double degenerate, which is commonly used, because the term double degenerate is sometimes used for white dwarf – neutron star or double neutron star binaries.

In this paper we present a new population synthesis for double white dwarfs, which is different from previous studies in three aspects. The first are some differences in the modelling of the binary evolution, in particular the description of a common envelope without spiral-in, in which the change in orbit is governed by conservation of angular momentum, rather than of energy (Sect. 2). The second new aspect is the use of detailed models for the cooling of white dwarfs (Sect. 4.3), which are important because it is the rate of cooling which to a large extent determines how long a white dwarf remains detectable in a magnitude-limited observed sample. The third new aspect is that we use different models of the star formation history (Sect. 5). Results are presented in Sect. 6 and discussed in Sect. 7. The conclusions are summarised in Sect. 8. In the Appendix some details of our population synthesis are described.

2. Binary and single star evolution; the formation of double white dwarfs

The code we use is based on the code described by Portegies Zwart & Verbunt (1996) and Portegies Zwart & Yungelson (1998), but has been modified in two respects; the white dwarf masses and the treatment of unstable mass transfer.

2.1. White dwarf masses

The masses of white dwarfs in binaries provide important observational constraints on evolution models. Therefore we have improved the treatment of the formation of white dwarfs in our binary evolution models by keeping more accurate track of the growth of the mass of the core. Details are given in Appendix A.1.1.

2.2. Unstable mass transfer

There exist two "standard" scenarios for the formation of close double white dwarfs. In the first, the binary experiences two stages of unstable mass transfer in which a common envelope is formed. The change of the binary orbital separation in a common envelope is treated on the base of a balance between orbital energy and the binding energy of the envelope of the mass-losing star (Paczyński 1976; Tutukov & Yungelson 1979; Webbink 1984; Iben & Livio 1993). The second scenario assumes that the first-born white dwarf of the pair is formed via stable mass transfer, like in Algol-type binaries (possibly accompanied by some loss of mass and angular momentum from the system) and the second white dwarf is formed via a common envelope.

Reconstruction of the evolution of three double helium white dwarfs with known masses of both components led us to the conclusion that a spiral-in could be avoided in the first phase of unstable mass transfer (Nelemans et al. 2000). Briefly, when the mass ratio of two stars entering a common envelope is not too far from unity, we assume that the envelope of the evolving giant is ejected without a spiral-in, and that the change in orbital separation is governed by conservation of angular momentum (the equation used is given in Appendix A.2.3). We parametrise the loss of angular momentum from the binary with a factor γ. If the mass ratio is more extreme, the common envelope leads to a spiral-in, which is governed by the conservation of energy (the equation used is given in Appendix A.2.2). The efficiency with which the energy of the binary orbit is used to expell the envelope of the giant is parametrised by a factor $\alpha_{\rm ce}\lambda$. We switch between the two descriptions at the mass ratio where both give the same change of the separation (roughly at 0.2). Nelemans et al. (2000) find that values of $\gamma = 1.75$ and $\alpha_{\rm ce}\lambda = 2$ give the best agreement of evolution models with the observed parameters of three binaries in which the masses of both white dwarfs are known, and therefore we use these values in our calculations.

Another novelty is what we suggest to call *"double spiral-in"* (see Brown 1995). It describes the situation when the primary fills its Roche lobe at the time that its companion has also evolved off the main sequence. This kind of evolution can only take place when the initial mass ratio is close to unity. Such a mass transfer phase has hitherto been described with the standard common envelope formalism; in the same way as when the companion is still a main sequence star. However, if the companion is evolved, one might as well argue that the envelope of the smaller star becomes part of the common envelope, and the envelopes of *both* stars will be expelled. We propose to use the energy balance here, since the double core binary will in general not have enough angular momentum to force the envelope into co-rotation. An equation for the change in orbital separation in the case of a "double spiral-in" is derived in Appendix A.2.4 exactly analogous to the usual common envelope formalism (e.g. Webbink 1984).

2.3. Examples

Before discussing effects that influence the double white dwarf population as a whole we discuss some typical examples of binary evolution leading to close double white dwarfs, to illustrate some of the assumptions used in our models. For details of the treatment of binary evolution we refer to Portegies Zwart & Verbunt (1996) and the Appendix.

2.3.1. Double helium white dwarfs

The most common double white dwarfs consist of two helium white dwarfs (Sect. 6.1). These white dwarfs descend from systems in which both stars have $M \lesssim 2.3\,M_\odot$ and fill their Roche lobes before He ignition in their degenerate cores. In Fig. 1 (top left) we show an example of the formation of such a system. We start with a binary with an orbital period of 40 days and components of 1.4 and 1.1 $M_\odot$. The primary fills its Roche lobe after 3 Gyrs,

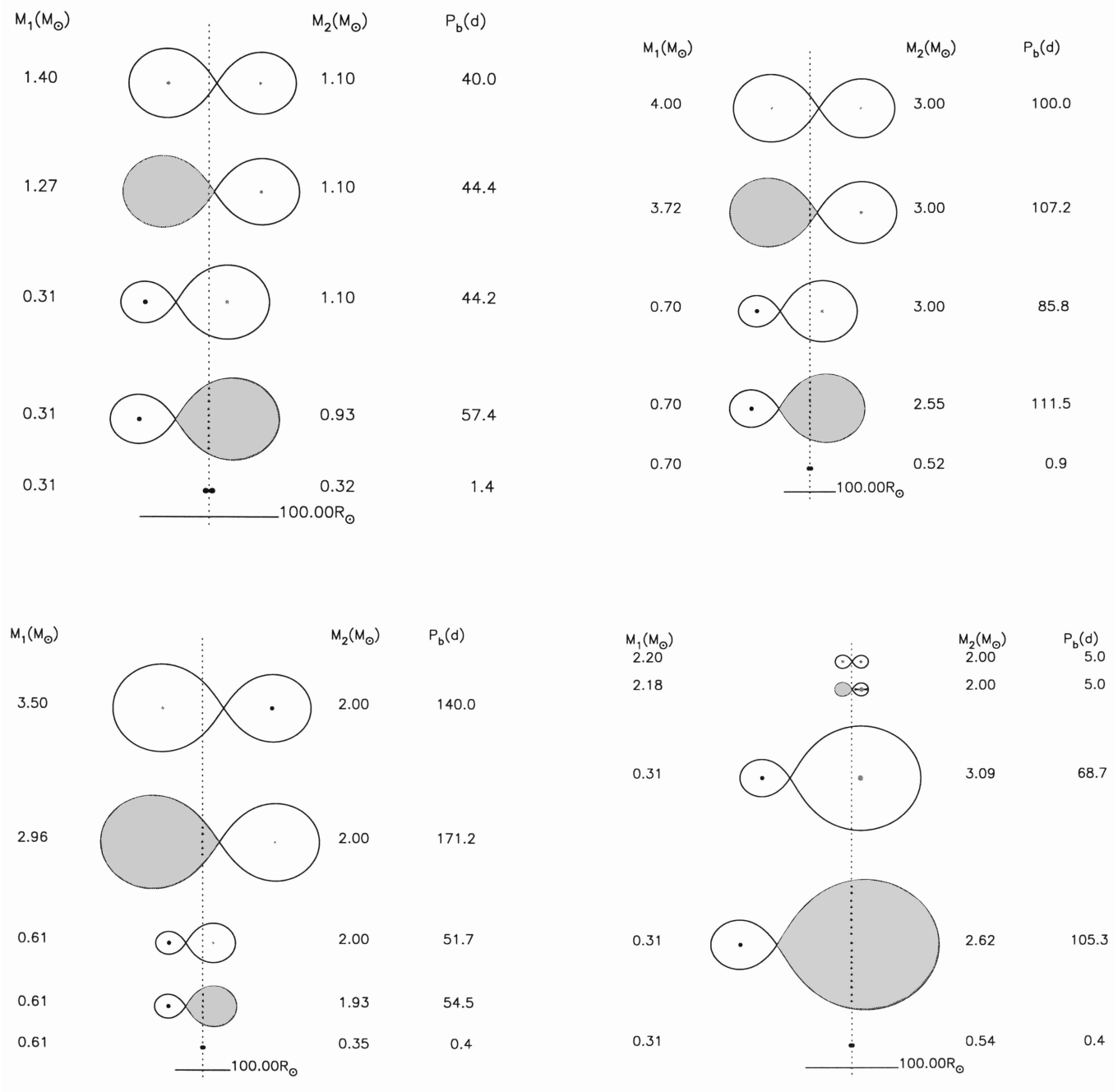

Fig. 1. Evolutionary scenarios for the formation of a double helium white dwarf (top left), a double CO white dwarf (top right) and the CO+He and He+CO pairs (bottom ones). Note that the scales in the panels differ as indicated by the 100 $R_\odot$ rulers at the bottom. For a more detailed discussion see Sect. 2.3

at which moment it has already evolved up the first giant branch and has lost $\sim$0.13 $M_\odot$ in a stellar wind. When the star fills its Roche lobe it has a deep convective envelope, so the mass transfer is unstable. We apply the envelope ejection formalism to describe the mass transfer with a γ-value of 1.75 (see Eq. (A.16)). The core of the donor becomes a 0.31 $M_\odot$ helium white dwarf. The orbital period of the system hardly changes. After 4 Gyr, when the first formed white dwarf has already cooled to very low luminosity, the secondary fills its Roche lobe and has a deep convective envelope. Mass loss again proceeds on dynamical time scale, but the mass ratio of the components is rather extreme and a common envelope is formed in which the orbit shrinks dramatically.

2.3.2. Double CO white dwarfs

Most double CO white dwarfs are formed in systems which are initially so wide that both mass transfer phases take place when the star is on the AGB and its core consists already of CO, such that a CO white dwarfs are formed directly. An example is shown in Fig. 1 (top right). In the first phase of mass transfer the change of the orbital separation is regulated by the conservation of angular momentum during envelope ejection, according to Eq. (A.16), while in the second phase of mass transfer spiral-in is described by Eq. (A.14).

Much less frequently, CO white dwarfs are formed by stars more massive than $2.3\,M_\odot$ which fill their Roche lobe when they have a nondegenerate core, before helium ignition. Roche lobe overflow then results in the formation of a low-mass helium star. A brief additional phase of mass transfer may happen, if the helium star expands to giant dimensions during helium shell burning. This is the case for $0.8 \lesssim M_{\rm He}/M_\odot \lesssim 3$ (see Appendix A.1.2). After exhaustion of helium in its core, the helium star becomes a CO white dwarf.

2.3.3. CO white dwarfs with He companions

In Fig. 1 (bottom left) we show an example in which the CO white dwarf is formed first. It starts with a more extreme mass ratio and a relatively wide orbit, which shrinks in a phase of envelope ejection. The secondary does not accrete anything and fills its Roche lobe when it ascends the first giant branch, having a degenerate helium core. It then evolves into a helium white dwarf.

In the second example (shown in Fig. 1; bottom right), the system evolves through a stable mass exchange phase because the primary has a radiative envelope when it fills its Roche lobe. Part of the transferred mass is lost from the system (see Appendix A.2.1). The orbit widens and the primary forms a helium white dwarf when it has transferred all its envelope to its companion. The secondary accretes so much mass that it becomes too massive to form a helium white dwarf. The secondary fills its Roche lobe on the AGB to form a CO white dwarf in a common envelope in which the orbital separation reduces strongly. Because of the differential cooling (Sect. 4.3) the CO white dwarf, despite the fact that it is formed last, can become fainter than its helium companion. Since the probability to fill their Roche lobe when the star has a radiative envelope, is low for low-mass stars, the scenario in which the helium white dwarf is formed first is less likely (see Sect. 6).

3. A model for the current population of white dwarfs in the Galaxy

We model the current population of double and single white dwarfs in the Galaxy using population synthesis and compare our models with the observed population. We initialise 250 000 "zero-age" binaries and evolve these binaries according to simplified prescriptions for single and binary star evolution, including stellar wind, mass transfer (which may involve loss of mass and angular momentum from the binary), common envelopes and supernovae.

Table 1. Models and their parameters. The IMF is always according to Miller & Scalo (1979). The SFR is either exponentially decaying (Eq. (4)) or constant. The column "% binaries" gives the initial binary fraction in the population, the column "cooling" gives the cooling model (see Sect. 4.3)

Model	SFH	% binaries	cooling
A1	Exp	50	DSBH98
A2	Exp	50	Modified DSBH98
A3	Exp	50	100 Myr
B	Exp	100	Modified DSBH98
C	Cnst	50	Modified DSBH98
D	Cnst	100	Modified DSBH98

For each initial binary the mass $M_{\rm i}$ of the more massive component, the mass ratio $q_{\rm i} \equiv m_{\rm i}/M_{\rm i} \leq 1$, where $m_{\rm i}$ is the mass of the less massive component, the orbital separation $a_{\rm i}$ and eccentricity $e_{\rm i}$ are chosen randomly from distributions given by

$$\begin{aligned} &\mathrm{Prob}(M_{\rm i}) && \text{MS79} && \text{for} && 0.96\,M_\odot \leq M_{\rm i} \leq 11\,M_\odot, \\ &\mathrm{Prob}(q_{\rm i}) \propto && \text{const.} && \text{for} && 0 < q_{\rm i} \leq 1, \\ &\mathrm{Prob}(a_{\rm i}) \propto && a_{\rm i}^{-1} && \text{for} && 0 \leq \log a_{\rm i}/R_\odot \leq 6, \\ &\mathrm{Prob}(e_{\rm i}) \propto && 2e_{\rm i} && \text{for} && 0 \leq e_{\rm i} \leq 1. \end{aligned} \quad (1)$$

For the primary mass we use the approximation of Eggleton et al. (1989) to the Miller & Scalo (1979) IMF indicated as MS79. A primary at the lower mass limit has a main sequence life time equal to our choice of the age of the Galactic disk (10 Gyr). The lower mass of less massive component is set to $0.08\,M_\odot$, the minimum mass for hydrogen core burning. The distribution over separation is truncated at the lower end by the separation at which the ZAMS binary would be semi-detached.

To investigate the effects of different cooling models (Sect. 4.3) and different assumptions about the star formation history (Sect. 5) different models have been computed (Table 1).

4. Modelling the observable population; white dwarf cooling

To model the observable population we have to take orbital evolution and selection effects into account.

4.1. Orbital evolution of double white dwarfs

The most important effect of orbital evolution, which is taken into account also in all previous studies of close binary white dwarfs, is the disappearance from the sample of the tightest systems as they merge, due to the loss of angular momentum via gravitational wave radiation. For example an $0.6\,M_\odot + 0.6\,M_\odot$ white dwarf pair with orbital period of 1 hour merges in $3\ 10^7$ yr. If it is located at a

distance of 100 pc from the Sun it will disappear abruptly from a magnitude limited sample by merging[2] before the white dwarfs have become undetectable due to cooling.

4.2. Selection effects

The observed double white dwarfs are a biased sample. First, they were mainly selected for study because of their supposed low mass, since this is a clear indication of binarity (Saffer et al. 1988; Marsh et al. 1995). Secondly, for the mass determinations and the measurement of the radial velocities the white dwarfs must be sufficiently bright. A third requirement is that the radial velocities must be large enough that they can be found, but small enough that spectral lines don't get smeared out during the integration. Maxted & Marsh (1999) discuss this last requirement in detail. Following them, we include a detection probability in the model assuming that double white dwarfs in the orbital period range between 0.15 hr and 8.5 day will be detected with 100% probability and that above 8.5 day the detection probability decreases linearly from 1 at 8.5 days to 0 at ∼35 days (see Fig. 1 in Maxted & Marsh 1999).

The second selection effect is related to the brightness of the white dwarfs, which is governed by their cooling curves.

4.3. White dwarf cooling

Iben & Tutukov (1985) noticed that for a $0.6\,M_\odot$ white dwarf the maximum probability of discovery corresponds to a cooling age of $\sim 10^8$ yr. In absence of detailed cooling curves for low-mass white dwarfs, it was hitherto assumed in population synthesis studies that white dwarfs remain bright enough to be observed during 10^8 yr, irrespective of their mass. However, recent computations (Blöcker 1995; Driebe et al. 1998, hereafter DSBH98; Hansen 1999) indicate that helium white dwarfs cool more slowly than CO white dwarfs, for two reasons. First, helium cores contain a higher number of ions than carbon-oxygen cores of the same mass, they store more heat and are brighter at the same age (Hansen 1999). Second, if the mass of the hydrogen envelope of the white dwarf exceeds a critical value, pp-reactions remain the main source of energy down to effective temperatures well below 10^4 K (Webbink 1975; DSBH98; Sarna et al. 2000). This residual burning may lead to a significant slow-down of the cooling.

White dwarfs in close binaries form when the evolution of (sub)giants with degenerate cores and hydrogen-rich envelopes is terminated by Roche lobe overflow. The amount of hydrogen that is left on the white dwarf depends on the details of this process. Fully fledged evolutionary calculations of the formation of helium white dwarfs, e.g. Giannone & Giannuzzi (1970); Sarna et al. (2000), as well as calculations that mimic Roche lobe overflow by mass loss at fixed constant rate (Driebe et al. 1998), find that the thickness of the residual envelope around the white dwarf is increasing with decreasing white dwarf mass. As a result the brightness at fixed age decreases monotonically with increasing white dwarf mass (see also Fig. A.2).

However, it is not clear that these calculations are valid for white dwarfs formed in a common envelope. In addition, white dwarfs may lose mass by stellar wind when they still have a high luminosity. Such winds are observed for nuclei of planetary nebulae and post-novae and could also be expected for He white dwarfs. Finally, white dwarfs with masses between ∼0.2 and $\sim 0.3\,M_\odot$ experience thermal flashes (Kippenhahn et al. 1968; Webbink 1975; Iben & Tutukov 1986b; Driebe et al. 1999; Sarna et al. 2000), in which the envelopes expand. This may lead to additional mass loss in a temporary common envelope, especially in the closest systems with separations $\lesssim 1\,R_\odot$. Mass loss may result in extinguishing of hydrogen burning (Iben & Tutukov 1986b; Sarna et al. 2000).

Hansen (1999) argues that the details of the loss of the hydrogen envelope are very uncertain and assumes that all white dwarfs have a hydrogen envelope of the same mass. He finds that helium white dwarfs cool slower than the CO white dwarfs, but inside these groups, the more massive white dwarfs cool the slowest. The difference within the groups are small.

We conclude that the cooling models are still quite uncertain, so we will investigate the result of assuming different cooling models in our population synthesis.

The first model we compute (A1; see Table 1 for a list of all computed models) uses the cooling curves as given by Blöcker (1995) for CO white dwarfs and DSBH98 for He white dwarfs as detailed in Appendix A.1.5. For the second model (A2) we made a crude estimate of the cooling curves for the case that the thermal flashes or a stellar wind reduce the mass of the hydrogen envelope and terminate the residual burning of hydrogen. We apply this to white dwarfs with masses below $0.3\,M_\odot$, and model all these white dwarfs identically and simply with cooling curves for a more massive (faster cooling) white dwarf of $0.46\ M_\odot$. To compare with the previous investigators, we include one model (A3) in which all white dwarfs can be seen for 100 Myrs. We did not model the cooling curves of Hansen (1999), because no data for $L > 0.01\ L_\odot$ are given.

4.4. Magnitude limited samples and local space densities

To convert the total Galactic population to a local population and to compute a magnitude limited sample, we assume a distribution of all single and binary stars in the galactic disk of the form

$$\rho(R,z) = \rho_0\ \mathrm{e}^{-R/H}\ \mathrm{sech}(z/h)^2 \quad \mathrm{pc}^{-3} \tag{2}$$

where we use $H = 2.5$ kpc (Sackett 1997) and $h = 200$ pc, neglecting the age and mass dependence of h.

[2] Note, however, that just before merging white dwarfs may become quite bright due to tidal heating (Iben et al. 1998).

To construct a magnitude limited sample, we compute the magnitude for all model systems from the cooling curves and estimate the contribution of each model system from Eq. (2). The absolute visual magnitudes along the cooling curves are derived using bolometric corrections after Eggleton et al. (1989).

From Eq. (2) the local ($R = 8.5$ kpc, $z = 30$ pc) space density ($\rho_{i,\odot}$) of any type of system is related to the total number in the Galaxy (N_i) by:

$$\rho_{i,\odot} = N_i / 4.8\ 10^{11} \quad \mathrm{pc}^{-3}. \tag{3}$$

5. Star formation history

Some progenitors of white dwarfs are formed long ago. Therefore the history of star formation in the Galaxy affects the contribution of old stars to the population of local white dwarfs. To study this we compute different models.

For models A and B (see Table 1), we model the star formation history of the galactic disk as

$$\mathrm{SFR}(t) = 15\ \exp(-t/\tau) \quad M_\odot\ \mathrm{yr}^{-1} \tag{4}$$

where $\tau = 7$ Gyr. It gives a current rate of $3.6\,M_\odot$ yr^{-1} which is compatible with observational estimates (Rana 1991; van den Hoek & de Jong 1997). The integrated SFR, i.e. the amount of matter that has been turned into stars over the whole history of the galactic disk (10 Gyr) with this equation is $\sim 8\ 10^{10}\ M_\odot$ which is higher than the current mass of the disk, since part of the gas that is turned into stars is given back to the ISM by supernovae and stellar winds.

For models C and D we use a constant SFR of $4\,M_\odot$ yr^{-1} (as Tutukov & Yungelson 1993). We use an age of the disk of 10 Gyr, while Tutukov & Yungelson (1993) use 15 Gyr. Model D also allows us to compare our results with previous studies (ITY97 and HAN98; see Sect. 7).

Most binary population synthesis calculations take a binary fraction of 100%. Since we want to compare our models with the observed fraction of close double white dwarfs among all white dwarfs, we present models with 100% binaries (models B and D); and with 50% binaries and 50% single stars, i.e. with 2/3 of all stars in binaries (models A and C).

6. Results

Our results are presented in the next subsections. In Sect. 6.1 we give the birth rates and total number of double white dwarfs in the Galaxy. These numbers allow a detailed comparison with results of earlier studies, which we defer to Sect. 7. They cannot be compared with observations directly, with the exception of the SN Ia rate. For comparison with the observed sample, described in Sect. 6.2, we compute magnitude limited samples in the remaining sections. In Sect. 6.3 the distribution over periods and masses is compared with the observations, which constrains the cooling models. Comparison of the mass ratio distribution with the observations gives further support for our new description of a common envelope without spiral-in (Sect. 6.4). In Sect. 6.5 we compare our model with the total population of single and binary white dwarfs and in Sect. 6.6 we compare models that differ in the assumed star formation history with the observed rate of PN formation and the local space density of white dwarfs.

6.1. Birth rates and numbers

In Table 2 the birth rates for all models are given. According to Eq. (1) the mass of a binary is on average 1.5 times the mass of a single star. For each binary in models A and C we also form a single star, i.e. per binary a total of 2.5 times the mass of a single star is formed (1.5 for the binary, 1 for the single star). For models B and D only 1.5 times the mass of a single star is formed per binary. Thus for the same SFR in $M_\odot$ yr^{-1} the frequency of each process involving a binary of the models A and C is 0.6 times that in models B and D.

For model A the current birth rate for close double white dwarfs is $4.8\ 10^{-2}$ yr^{-1} in the Galaxy. The expected total population of close binary white dwarfs in the galactic disk is $\sim 2.5\ 10^8$ (see Table 2).

The double white dwarfs are of the following types: 53% contains two helium white dwarfs; 25% two CO white dwarfs; in 14% a CO white dwarf is formed first and a helium white dwarf later and in 6% a helium white dwarf is formed followed by the formation of a CO white dwarf. The remaining 1% of the double white dwarfs contains an ONeMg white dwarf. The CO white dwarfs can be so called hybrid white dwarfs; having CO cores and thick helium envelopes (Iben & Tutukov 1985, 1987). Of the double CO white dwarfs, 6% contains one and 5% two hybrid white dwarfs. In the mixed pairs the CO white dwarf is a hybrid in 20% of the cases.

Forty eight percent of all systems are close enough to be brought into contact within a Hubble time. Most are expected to merge. The estimated current merger rate of white dwarfs is $2.2\ 10^{-2}$ yr^{-1}. The current merger rate of pairs that have a total mass larger than the Chandrasekhar limit ($M_{\mathrm{Ch}} = 1.44\,M_\odot$) is $3.2\ 10^{-3}\,\mathrm{yr}^{-1}$. Since the merging of binary CO white dwarfs with a combined mass in excess of M_{Ch} is a viable model for type Ia SNe (see Livio 1999, for the most recent review), our model rate can be compared with the SN Ia rate of $\sim(4\pm1)$ $10^{-3}\,\mathrm{yr}^{-1}$ for Sbc type galaxies like our own (Cappellaro et al. 1999). In 19% of the systems that come into contact the ensuing mass transfer is stable and an interacting double white dwarf (identified with AM CVn stars) is formed. The model birth rate of AM CVn systems is $4.6\ 10^{-3}$ yr^{-1} (see Table 2).

6.2. Observed sample of double white dwarfs

The properties of the observed double white dwarfs with which we will compare our models are summarised in

Table 2. Birth and event rates and numbers for the different models. All birth and event rates (ν) are in units of yr^{-1} in the Galaxy. All numbers (#) are total numbers in the Galaxy. Close double white dwarfs are represented with (wd, wd). See Sect. 6.1 for a discussion of these rates. For comparison (in Sect. 7.1) we also include numbers computed by the code from ITY97 but using an age of the galactic disk of 10 Gyr instead of the 15 Gyr used by ITY97; and numbers of model 1 of HAN98

Model	SFH	% bin	$\nu_{(\mathrm{wd,wd})}$ (10^{-2})	ν_{merge} (10^{-2})	SN Ia (10^{-3})	ν_{AMCVn} (10^{-3})	#(wd, wd) (10^{8})
A	Exp	50	4.8	2.2	3.2	4.6	2.5
B	Exp	100	8.1	3.6	5.4	7.8	4.1
C	Cnst	50	3.2	1.6	3.4	3.1	1.2
D	Cnst	100	5.3	2.8	5.8	5.2	1.9
ITY97[1]	Cnst	100	8.7	2.4	2.7	12.0	3.5
HAN98[1]	Cnst	100	3.2	3.1	2.9	26	1.0

[1] Note that ITY97 and HAN98 used a normalisation that is higher than we use for model D by factors ∼1.4 and ∼1.1 respectively (see Sect. 7.1).

Table 3. Parameters of known close double white dwarfs (first 14 entries) and subdwarfs with white dwarf companions. m denotes the mass of the visible white dwarf or subdwarf. The mass ratio q is defined as the mass of the brighter star of the pair over the mass of the companion. For references see Maxted & Marsh (1999); Moran et al. (1999); Marsh (1999); and Maxted et al. (2000). The mass of 0136+768 is corrected for a misprint in Maxted & Marsh (1999), for 0135+052 the new mass given in Bergeron et al. (1997) is taken. Data for the sdB star KPD 0422+5421 are from Oroz & Wade (1999) and for KPD 1930+2752 from Maxted et al. (2000). The remaining sdB stars do not have reliable mass estimates

WD/sdB	P(d)	q	m	sdB	P(d)
0135−052	1.556	0.90	0.25	0101+039	0.570
0136+768	1.407	1.31	0.44	0940+068	8.33
0957−666	0.061	1.14	0.37	1101+249	0.354
1022+050	1.157		0.35	1432+159	0.225
1101+364	0.145	0.87	0.31	1538+269	2.50
1202+608	1.493		0.40	2345+318	0.241
1204+450	1.603	1.00	0.51		
1241−010	3.347		0.31		
1317+453	4.872		0.33		
1704+481A	0.145	0.7	0.39		
1713+332	1.123		0.38		
1824+040	6.266		0.39		
2032+188	5.084		0.36		
2331+290	0.167		0.39		
KPD 0422+5421	0.090	0.96	0.51		
KPD 1930+2752	0.095	0.52	0.5		

Table 3. Only WD 1204+450 and WD 1704+481 are likely to contain CO white dwarfs, having components with masses higher than $0.46\,M_\odot$; the limiting mass to form a helium white dwarf (Sweigart et al. 1990). The remaining systems are probably helium white dwarfs. In principle in the mass range $M \simeq 0.35 - 0.45\,M_\odot$ white dwarfs could also be hybrid; however in this range the probability for a white dwarf to be hybrid is 4–5 times lower than to be a helium white dwarf, because hybrid white dwarfs originate from more massive stars which fill their Roche lobe in a narrow period range (see, however, an example of such a scenario for WD 0957−666 in Nelemans et al. 2000). We assume $0.05\,M_\odot$ for the uncertainty in the estimates of the masses of white dwarfs, which may be somewhat optimistic.

Table 3 also includes data on subdwarf B stars with suspected white dwarf companions. Subdwarf B (sdB) stars are hot, helium rich objects which are thought to be helium burning remnants of stars which lost their hydrogen envelope. When their helium burning has stopped they will become white dwarfs. Of special interest are KPD 0422+5421 (Koen et al. 1998; Orosz & Wade 1999) and KPD1930+2752 (Maxted et al. 2000). With orbital periods as short as 0.09 and 0.095 days, respectively, their components will inevitably merge. In both systems the sdB components will become white dwarfs before the stars merge. In KPD 1930+2752 the total mass of the components is close to the Chandrasekhar mass or even exceeds it. That makes this system the only currently known candidate progenitor for a SN Ia.

6.3. Period-mass distribution; constraints on cooling models

The observed quantities that are determined for all double white dwarfs are the orbital period and the mass of the brighter white dwarf. Following Saffer et al. (1998), we plot in Fig. 2 the $P_{\mathrm{orb}} - m$ distributions of the frequency of occurrence for the white dwarfs which are born at this moment and for the simulated magnitude limited sample for the models with different cooling prescriptions, (models A1, A2 and A3; see Table 1), where we assume $V_{\mathrm{lim}} = 15$ as the limiting magnitude of the sample[3]. For m we always use the mass of the brighter white dwarf. In general the brighter white dwarf is the one that was formed last, but occasionally, it is the one that was formed first as explained in Sect. 2.3.3. For comparison, we also plot the observed binary white dwarfs in Fig. 2.

[3] The $P - m$ distribution does not qualitatively change if we increase V_{lim} by one or two magnitudes, since we still deal with very nearby objects.

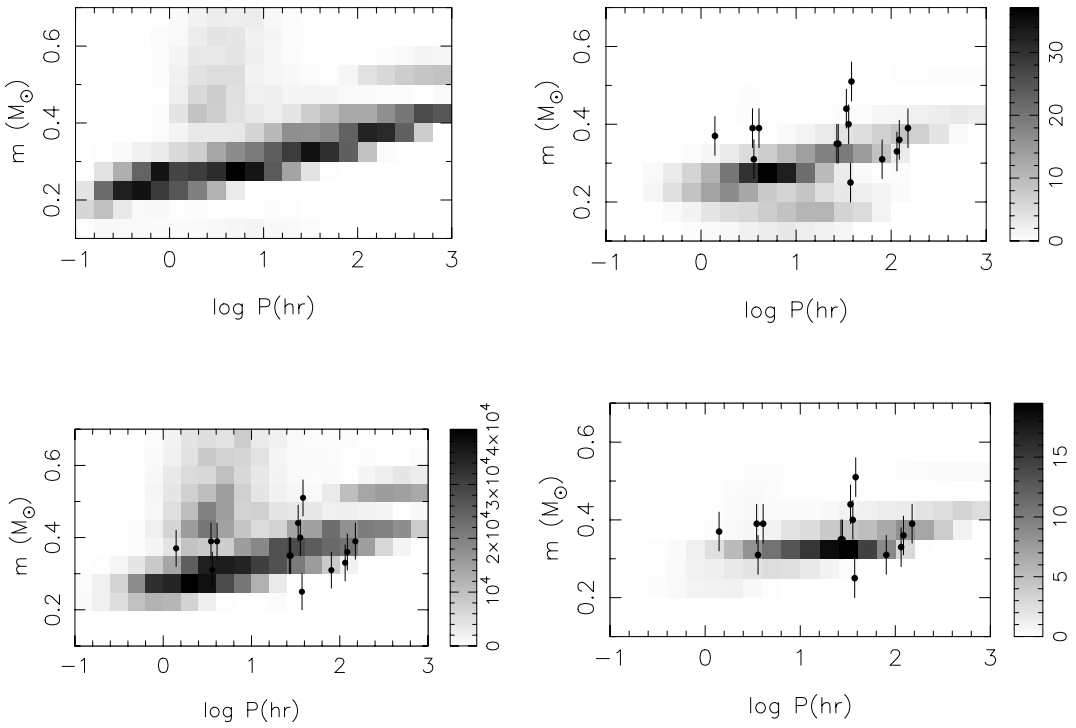

Fig. 2. Model population of double white dwarfs as function of orbital period and mass of the brighter white dwarf of the pair. Top left: distribution of the double white dwarfs that are currently born for models A. This is independent of cooling. In the remaining three plots we show the currently visible population of double white dwarfs for different cooling models: (top right) cooling according to DSBH98 and Blöcker (1995, model A1); (bottom right) cooling according to DSBH98, but with faster cooling for WD with masses below $0.3\,M_\odot$ (model A2). Both plots are for a limiting magnitude $V_{\rm lim} = 15$; (bottom left) with constant cooling time of 100 Myr (model A3, note that in this case we only obtain the *total number of potentially visible double white dwarfs in the Galaxy* and we cannot construct a magnitude limited sample). For comparison, we also plot the observed binary white dwarfs

There is a clear correlation between the mass of newborn low-mass (He) white dwarf and the orbital period of the pair. This can be understood as a consequence of the existence of a steep core mass–radius relation for giants with degenerate helium cores (Refsdal & Weigert 1970). Giants with more massive cores (forming more massive white dwarfs) have much larger radii and thus smaller binding energies. To expell the envelope in the common envelope, less orbital energy has to be used, leading to a larger orbital period. The spread in the distribution is caused by the difference in the masses of the progenitors and different companion masses.

In the simulated population of binary white dwarfs there are three distinct groups of stars: He dwarfs with masses below $0.45\,M_\odot$, hybrid white dwarfs with masses in majority between 0.4 and 0.5 $M_\odot$ and periods around a few hours, and CO ones with masses above $0.5\,M_\odot$. The last groups are clearly dominated by the lowest mass objects. The lowest mass CO white dwarfs are descendants of most numerous initial binaries with masses of components 1–2 $M_\odot$.

The different cooling models result in very different predicted observable distributions. Model A1 where the cooling curves of DSBH98 are applied favours low mass white dwarfs to such an extent that almost all observed white dwarfs are expected to have masses below $0.3\,M_\odot$. This is in clear contrast with the observations, in which all but one white dwarf have a mass above $0.3\,M_\odot$. Reduced cooling times for white dwarfs with masses below $0.3\,M_\odot$ (model A2) improves this situation. Model A3, with a constant cooling time (so essentially only affected by merging due to GWR), seems to fit all observed systems also nicely. However, a complementary comparison with the observations as given by cumulative distributions of the periods (Fig. 3), shows that model A2 fits the data best, and that model A3 predicts too many short period systems.

The observed period distribution for double white dwarfs shows a gap between 0.5 and 1 day, which is not present in our models. If we include also sdB binaries, the gap is partially filled in. More systems must be found to determine whether the gap is real.

The comparison of our models with observations suggests that white dwarfs with masses below $0.3\,M_\odot$ cool faster than predicted by DSBH98. Mass loss in thermal flashes and a stellar wind may be the cause of this.

The model sample of detectable systems is totally dominated by He white dwarfs with long cooling times. Given our model birth rates and the cooling curves we apply, we estimate the number of double white dwarfs to be detected in a sample limited by $V_{\rm lim} = 15$ as 220 of which

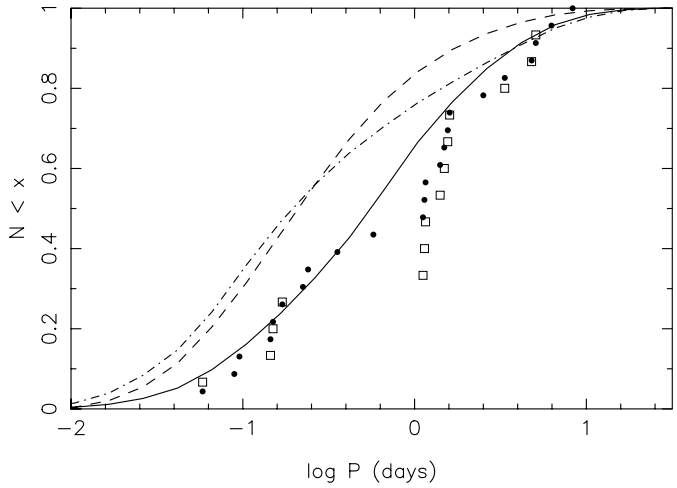

Fig. 3. Cumulative distribution of periods. Solid line for our best model (A2); DSBH98 cooling, but with lower luminosity due to thermal flashes for white dwarfs with masses below $0.3\,M_\odot$. Dashed line for DSBH98 without modifications (model A1) and dash dotted line for constant cooling time of 100 Myr (model A3). Open squares for the observed double white dwarfs, filled circles give the observed systems including the sdB binaries (Table 3)

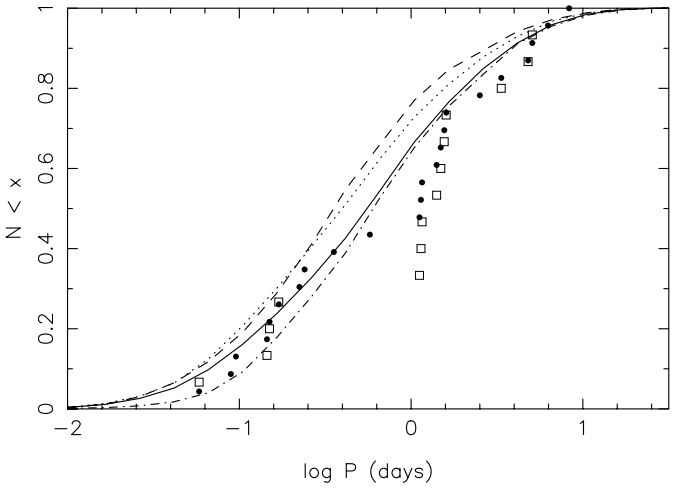

Fig. 4. Cumulative distribution of periods. Solid line for model A2 as in Fig. 3, dashed line for the same model but with $\alpha_{\rm ce}\lambda = 1$, dash-dotted line for a model with $\gamma = 1.5$ and finally the dotted line for model C (constant SFR)

Table 4. Number of observable white dwarfs, close double white dwarfs and SN Ia progenitors as function of the limiting magnitude of the sample for model A2

$V_{\rm lim}$	#wd	#wdwd	#SN Ia prog
15.0	855	220	0.9
15.5	1789	421	1.7
16.0	3661	789	3.2
17.0	12 155	2551	11.2

only 10 are CO white dwarfs for model A2. Roughly one of these is expected to merge within a Hubble time having a total mass above $M_{\rm Ch}$. For future observations we give in Table 4 a list of expected number of systems for different limiting magnitudes.

It should be noted that these numbers are uncertain. This is illustrated by the range in birth rates for the different models (Table 2) and by the differences with previous studies (see Sect. 7.1). Additional uncertainties are introduced by our limited knowledge of the initial distributions (Eq. (1)) and the uncertainties in the cooling and the Galactic model (Eq. (2)). For example Yungelson et al. (1994) compare models with two different $q_{\rm i}$ distributions (one peaked towards $q_{\rm i} \sim 1$) and show that the birth rates differ by a factor ∼1.7. In general the relative statistics of the model is more reliable than the absolute statistics.

Before turning to the mass ratio distribution, we illustrate the influence of the model parameters we choose. We do this by showing cumulative period distributions for some models with different parameters in Fig. 4; $\alpha_{\rm ce}\lambda = 1$ (dashed line) and $\gamma = 1.5$ (dash-dotted line). It shows that the change in parameters influences the distributions less than the different cooling models discussed above, although the observations favour a higher $\alpha_{\rm ce}\lambda$. We also included the cumulative distribution for model C (with a constant SFR; dotted line) which differs from that for model A2 in that it has fewer long period systems. This is a consequence of the larger relative importance of old, low-mass progenitor binaries in model A2, which lose less mass and thus shrink less in the first phase of mass transfer (see Eq. (A.16)).

6.4. Period-mass ratio distribution

Our assumption that a common envelope can be avoided in the first phase of mass transfer between a giant and a main-sequence star, is reflected in the mass ratios of the model systems. A clear prediction of the model is that close binary white dwarfs must concentrate to $q = m/M \sim 1$. For the observed systems, the mass ratio can only be determined if both components can be seen, which in practice requires that the luminosity of the fainter component is more than 20% of that of the brighter component (Moran et al. 2000). Applying this selection criterium to the theoretical model, we obtain the distribution shown in Fig. 5 for the magnitude limited sample. Note that since lower mass white dwarfs cool slower this selection criterion favours systems with mass ratios above unity. In the same figure we also show the observed systems.

For comparison we also computed a run (A′) in which we used the standard common envelope treatment for the first phase of mass transfer, which is done by ITY97 and HAN98. The fraction of double white dwarfs for which the mass ratio can be determined according to the selection criterium of a luminosity ratio greater than 0.2, is 27% for model A2 and 24% for model A′. In a total of 14 systems one thus expects 4 ± 2 and 3 ± 2 systems of which the mass ratio can be determined. Model A2 fits the observed

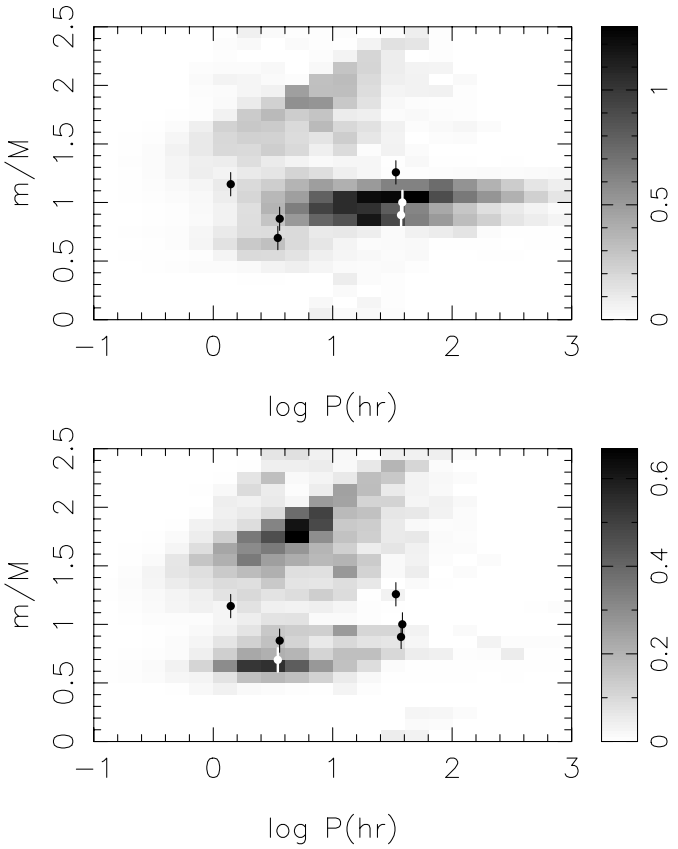

Fig. 5. Top: current population of double white dwarfs as function of orbital period and mass ratio, for model A2, a limiting magnitude of 15 and a maximal ratio of luminosities of 5. Bottom: the same for a run in which the first phase of mass transfer is treated as a standard common envelope, as is done by ITY97 and HAN98. For comparison, we also plot the observed binary white dwarfs

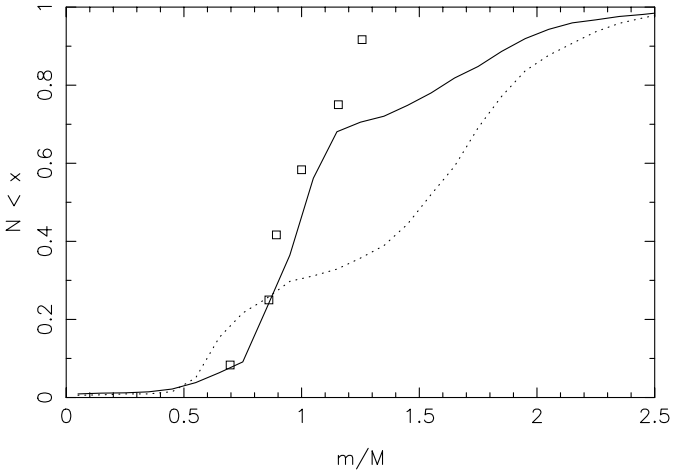

Fig. 6. Cumulative mass ratio distributions for the models A2 (solid line) and A′ (dotted line) as explained in Sect. 6.4. The observed mass ratio's are plotted as the open squares

number better, but the numbers are too small to draw conclusions. The distribution of mass ratios in model A′ (Fig. 5, bottom) however clearly does not describe the observations as well as our model A2, as illustrated in more detail in a plot where the cumulative mass ratio distributions of the two models and the observations are shown (Fig. 6).

6.5. Mass spectrum of the white dwarf population; constraints on the binary fraction

Figures 7 and 8 show the model spectrum of white dwarf masses for models B and A2, including both single and double white dwarfs for a limiting magnitude $V_{\rm lim} = 15$. For this plot we consider as "single" white dwarfs all objects that were born in initially wide pairs, single merger products, white dwarfs that became single as a result of binary disruption by SN explosions, white dwarfs in close pairs which are brighter than their main-sequence companions and genuine single white dwarfs for the models with an initial binary fraction smaller than 100%.

These model spectra can be compared to the observed mass spectrum of DA white dwarfs studied by Bergeron et al. (1992) and Bragaglia et al. (1995), shown in Fig. 9. The latter distribution may have to be shifted to higher masses by about $0.05\,M_\odot$, if one uses models of white dwarfs with thick hydrogen envelopes for mass estimates (Napiwotzki et al. 1999). Clearly, a binary fraction of 50% fits the observed sample better, if indeed helium white dwarfs cool much slower than CO white dwarfs. We can also compare the absolute numbers. Maxted & Marsh (1999) conclude that the fraction of close double white dwarfs among DA white dwarfs is between 1.7 and 19% with 95% confidence. For model B the fraction of close white dwarfs is ∼43% (853 white dwarfs of which 368 are close pairs), for model A2 is is ∼26% (855 white dwarfs and 220 close pairs). Note that this fraction slightly decreases for higher limiting magnitudes because the single white dwarfs are more massive and thus generally dimmer, sampling a different fraction of Galaxy. An even lower binary fraction apparently would fit the data better, but is in conflict with the estimated fraction of binaries among normal main sequence binaries (Abt 1983; Duquennoy & Mayor 1991). However this number highly depends on uncertain selection effects.

There are some features in the model mass spectrum in model A2 that appear to be in conflict with observations. The first is the clear trend that with the cooling models of DSBH98, even with our modifications, there should be an increasing number of helium white dwarfs towards lower masses. The observed distribution is flat. A very simple numerical experiment in which we assign a cooling curve to all helium white dwarfs as the one for a $0.414\,M_\odot$ white dwarf according to DSBH98 and a cooling curve as for a $0.605\,M_\odot$ white dwarf according to Blöcker (1995) for all CO white dwarfs (Fig. 10), shows that an equal cooling time for all helium white dwarfs seems to be in better agreement with the observations. It has a fraction of double white dwarfs of 18%.

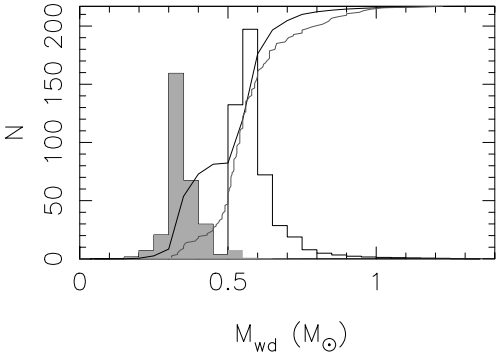

Fig. 7. Mass spectrum of all white dwarfs for model B (100% binaries). Members of close double white dwarfs are in grey. The cumulative distribution is shown as the solid black line. For comparison, the grey line shows the cumulative distribution of the observed systems (Fig. 9)

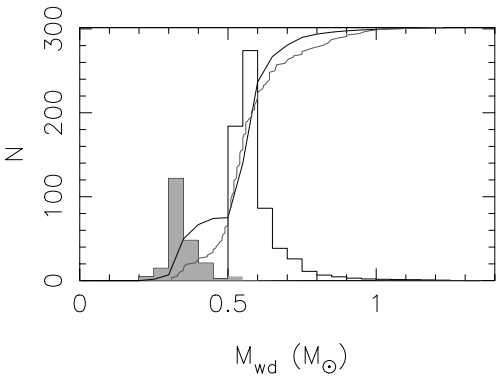

Fig. 8. Mass spectrum of all white dwarfs for model A2 (initial binary fraction of 50%) Double white dwarfs are in grey. The cumulative distribution is shown as solid black line and cumulative distribution of observed systems as the grey line

Another feature is the absence of stars with $0.45 \lesssim M/M_\odot \lesssim 0.5$ in the model distributions. This is a consequence of the fact that in this interval in our models only hybrid white dwarfs can be present, which have a low formation probability (see Sect. 6.2).

We conclude that an initial binary fraction of 50% can explain the observed close binary fraction in the white dwarf population. The shape of the mass spectrum, especially for the helium white dwarfs is a challenge for detailed mass determinations and cooling models.

6.6. Birth rate of PN and local WD space density; constraints on the star formation history

Finally, we compare models A and C (see Table 1), which differ only by the assumed star formation history. The star formation rate was probably higher in the past than at present and some (double) white dwarfs descend from stars that are formed just after the galactic disk was formed.

Table 5 gives the formation rates of PN and the total number of white dwarfs in the Galaxy for models A and C. The total number of white dwarfs is computed by excluding all white dwarfs in binaries where the companion is brighter. The local density of white dwarfs and PN rate are computed with Eq. (3) as described in Sect. 4.4.

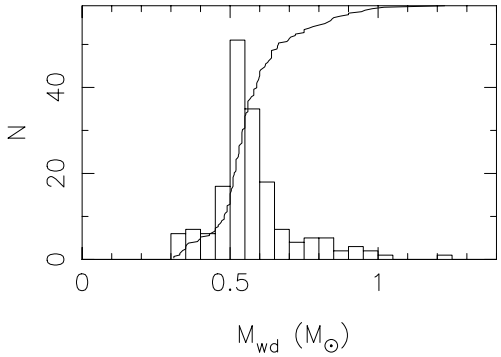

Fig. 9. Mass spectrum of observed white dwarfs. Data are taken from Bergeron et al. (1992) and Bragaglia et al. (1995). The solid line is the cumulative distribution

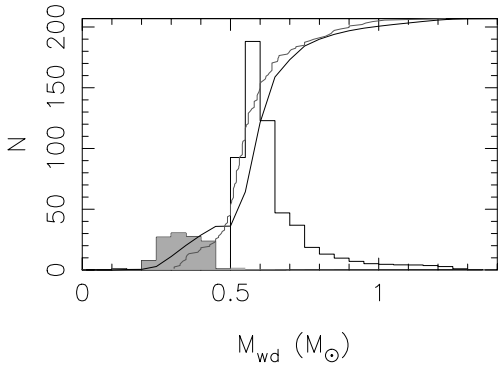

Fig. 10. Mass spectrum of all white dwarfs as in Fig. 8 in a model in which all helium white dwarfs cool like a $0.4\,M_\odot$ dwarf and all CO white dwarfs cool like a $0.6\,M_\odot$ white dwarf. Lines are cumulative distributions for the model (black) and the observations (grey)

Table 5. Galactic number and local space density of white dwarfs; and Galactic and local PN formation rate for the models A and C. Unit of the PN formation rates is yr^{-1}; unit for $\rho_{\mathrm{wd},\odot}$ is pc^{-3}. The ranges of observed values are given for comparison. For references and discussion see Sect. 6.6

Model	SFH	% bin	#wd 10^9	ν_{PN}	$\rho_{\mathrm{wd},\odot}$ (10^{-3})	$\nu_{\mathrm{PN},\odot}$ (10^{-12})
A	Exp	50	9.2	1.1	19	2.3
C	Const	50	4.1	0.8	8.5	1.7
Obs					4–20	3

We can compare these numbers with the observational estimates for the local PN formation rate of $3\ 10^{-12}\ \mathrm{pc}^{-3}\ \mathrm{yr}^{-1}$ (Pottasch 1996) and the local space density of white dwarfs, which range from e.g. $4.2\ 10^{-3}\ \mathrm{pc}^{-3}$ (Knox et al. 1999) through $7.6^{+3.7}_{-0.7}\ 10^{-3}\ \mathrm{pc}^{-3}$ (Oswalt et al. 1995) and $10\ 10^{-3}\ \mathrm{pc}^{-3}$ (Ruiz & Takamiya 1995) to $20 \pm 7\ 10^{-3}\ \mathrm{pc}^{-3}$ (Festin 1998).

This list shows the large uncertainty in the observed local space density of white dwarfs. It appears that the lower values are somewhat favoured in the literature. Both models A and C appear for the moment to be consistent with the observed local white dwarf space density and with the PN formation rate. However, we prefer model A2 since it fits the period distribution better (see Fig. 4).

The ratio of the local space density of white dwarfs to the current local PN formation rate could in principle serve as a diagnostic for the star formation history of the Galaxy, given better knowledge of $\rho_{\mathrm{wd},\odot}$, which critically depends on the estimates of the incompleteness of the observed white dwarf samples and the applied cooling curves.

7. Discussion: Comparison with previous studies

We now compare our work with the results of previous studies; in particular the most recent studies of Iben et al. (1997, ITY97) and Han (1998, HAN98).

7.1. Birth rates

In Table 2 we show the birth rates of close double white dwarfs for the different models. We also include numbers from HAN98 (model 1) and a set of numbers computed with the same code as used in ITY97, but for an age of the galactic disk of 10 Gyr, as in our models. The numbers of HAN98 are for an age of the disk of 15 Gyr. Our model D is the closest to the models of ITY97 and HAN98, assuming a constant SFR and 100% binaries. To estimate the influence of the binary evolution models only in comparing the different models we correct for their different normalisations.

In the recomputed ITY97 model the formation rate of interacting binaries in which the primary evolves within the age of the Galaxy is 0.35 yr^{-1}. In our model D this number is 0.25 yr^{-1}. In the following we therefore multiply the formation rates of ITY97 as given in Table 2 with 0.71.

In the model of HAN98 one binary with a primary mass above 0.8 $M_\odot$ is formed in the Galaxy annually with $\log a_\mathrm{i} < 6.76$, i.e. 0.9 binary with $\log a_\mathrm{i} < 6$, which is our limit to a_i. Correcting for the different assumed age of the Galaxy we estimate this number to be 0.81; in our model this number is 0.73. We thus multiply the the formation rates of HAN98 as given in Table 2 with 0.9.

Applying these corrections to the normalisation, we find that some interesting differences remain. The birth rate of double white dwarfs is 0.029, 0.053 and 0.062 per year for HAN98, model D and ITY98 respectively. At the same time the ratio of the merger rate to the birth rate decreases: 0.97, 0.53 and 0.28 for these models. This can probably be attributed to the different treatment of the common envelope. HAN98 uses a common envelope spiral-in efficiency of 1 in Webbinks (1984) formalism, while we use 4 (for $\lambda = 0.5$, see De Kool et al. 1987). ITY97 use the formalism proposed by Tutukov & Yungelson (1979) with an efficiency of 1. This is comparable to an efficiency of 4–8 in the Webbink formalism. This means that in the model of HAN98, more systems merge in a common envelope, which yields a low formation rate of double white dwarfs. The ones that form (in general) have short periods for the same reason, so the ratio of merger to birth rate is high. In the ITY model the efficiency is higher, so more systems will survive both common envelopes and have generally wider orbits, leading to a much lower ratio of merger to birth rate. Our model D is somewhat in between, but also has the different treatment of the first mass transfer phase (Sect. 2), in which a strong spiral-in is avoided.

The difference between the models in the SN Ia rate ($\nu_{\mathrm{SN\ Ia}}$) is related both to the total merger rate and to the *masses* of the white dwarfs. The former varies within a factor ∼1.5: 0.017, 0.028, and 0.028 yr^{-1} for ITY97, model D, and HAN98, while $\nu_{\mathrm{SN\ Ia}}$ is higher by a factor 2–3 in model D compared to the other models. This is caused by the initial–final mass relation in our models, which is derived from stellar models with core overshooting, producing higher final masses.

The difference in the birthrate of interacting white dwarfs (ν_{AMCVn}) is mainly a consequence of our treatment of the first mass transfer, which gives for model D a mass ratio distribution which is peaked to 1 (Sect. 6.4), while in ITY97 and HAN98 the mass ratio is in general different from 1 (Sect. 7.2), favouring stable mass transfer and the formation of AM CVn systems. An additional factor, which reduces the number of AM CVn systems is the assumption in model D and ITY97 that the mass transfer rate is limited by the Eddington rate. The formation and evolution of AM CVn stars is discussed in more detail in Tutukov & Yungelson (1996) and Nelemans et al. (2001).

7.2. Periods, masses and mass ratios

Comparing our Fig. 2 with the corresponding figure in Saffer et al. (1998), we find the same trend of higher white dwarf masses at longer periods. However, in our model the masses are higher than in the model of Saffer et al. (1998) at the same period. This is a consequence of the absence of a strong spiral-in in the first mass transfer phase in our model, contrary to the conventional common envelope model, as discussed in 2.2.

In our model the mass ratio distribution is peaked at $q \approx 1$. This is different from the models of ITY97 and Saffer et al. (1998) which predict a strong concentration to $q \sim 0.5{-}0.7$ and from HAN98 who finds typical values of $q \sim 0.5$, with a tail to $q \sim 2$. The difference between these two latter groups of models may be understood as a consequence of enhanced wind in Han's model (see also Tout & Eggleton 1988), which allows wider separations before the second common envelope. The mass ratio distribution of our model, peaked at $q \simeq 1$, appears to be more consistent with the observed mass ratio distribution.

7.3. Cooling

To explain the lack of observed white dwarfs with masses below 0.3 $M_\odot$ we had to assume that these white dwarfs cool faster than predicted by the models of DSBH98.

The same assumption was required by Kerkwijk et al. (2000), to bring the cooling age of the white dwarf that accompanies PSR B1855+09 into agreement with the pulsar spin-down age; and to obtain cooling ages shorter than the age of the Galaxy for the white dwarfs accompanying PSR J0034−0534 and PSR J1713+0747.

The absence of the lowest mass white dwarfs could also be explained by the fact that a common envelope involving a giant with a low mass helium core ($M_c < 0.2$–$0.25\,M_\odot$) always leads to a complete merger, according to Sandquist et al. (2000). However it can not explain the absence of the systems with $0.25 < M < 0.3\,M_\odot$, which would form the majority of the observed systems using the full DSBH98 cooling (model A1; see Fig. 2).

8. Conclusions

We computed a model of the population of close binary white dwarfs and found good agreement between our model and the observed double white dwarf sample. A better agreement with observations compared to earlier studies is found due to two modifications.

The first is a different treatment of unstable mass transfer from a giant to a main sequence star of comparable mass. The second is a more detailed modelling of the cooling of low mass white dwarfs which became possible because detailed evolutionary models for such white dwarfs became available. Our main conclusions can be summarised as follows.

1. Comparing the mass distribution of the white dwarfs in close pairs with the observations, we find a lack of observed white dwarfs with masses below 0.3 $M_\odot$. This discrepancy can be removed with the assumption that low-mass white dwarfs cool faster than computed by Driebe et al. (1998). The same assumption removes discrepancies between observed and derived ages of low-mass white dwarfs that accompany recycled pulsars, as shown by van Kerkwijk et al. (2000). Faster cooling is expected if the hydrogen envelopes around low-mass white dwarfs are partially expelled by thermal flashes or a stellar wind;
2. Our models predict that the distribution of mass ratios of double white dwarfs, when corrected for observational selection effects as described by Moran et al. (2000), peaks at a mass ratio of unity, consistent with observations. The distributions predicted in the models by Iben et al. (1997) and Han (1998) peak at mass ratios of about 0.7 and above 1.5 and agree worse with the observations even after applying selection effects;
3. Our models predict a distribution of orbital periods and masses of close double white dwarfs in satisfactory agreement with the observed distribution;
4. Amongst the observed white dwarfs only a small fraction are members of a close pair. To bring our models into agreement with this, we have to assume an initial binary fraction of 50% (i.e. as many single stars as binaries);
5. In our models the ratio of the local number density of white dwarfs and the planetary nebula formation rate is a sensitive function of the star formation history of the Galaxy. Our predicted numbers are consistent with the observations;
6. Using detailed cooling models we predict that an observed sample of white dwarfs near the Sun, limited at the magnitude $V = 15$, contains 855 white dwarfs of which 220 are close pairs. Of these pairs only 10 are double CO white dwarfs and only one is expected to merge having a combined mass above the Chandrasekhar mass. The predicted merger rate in the Galaxy of double white dwarfs with a mass that exceeds the Chandrasekhar mass is consistent with the inferred SN Ia rate.
   ITY97 estimated, depending on α_{ce}, to find one such pair in a sample of ∼200 to ∼600 white dwarfs. Reversing this argument, when the statistics become more reliable, the observed number of systems with different types of white dwarfs could provide constraints on the cooling models for these white dwarfs.

Acknowledgements. We thank the referee A. Gould for valuable comments. LRY and SPZ acknowledge the warm hospitality of the Astronomical Institute "Anton Pannekoek". This work was supported by NWO Spinoza grant 08-0 to E. P. J. van den Heuvel, the Russian Federal Program "Astronomy" and RFBR grant 99-02-16037 and by NASA through Hubble Fellowship grant HF-01112.01-98A awarded (to SPZ) by the Space Telescope Science Institute, which is operated by the Association of Universities for Research in Astronomy, Inc., for NASA under contract NAS 5-26555.

Appendix A: Population synthesis code SeBa

We present some changes we made to the population synthesis code SeBa (see Portegies Zwart & Verbunt 1996; Portegies Zwart & Yungelson 1998).

A.1. Stellar evolution

As before, the treatment of stellar evolution in our code is based on the fits to detailed stellar evolutionary models (Eggleton et al. 1989; Tout et al. 1997), which give the luminosity and the radius of the stars as a function of time and mass. In addition to this we need the mass of the core and the mass loss due to stellar wind. These we obtain as follows.

A.1.1. Core masses and white dwarf masses

For the mass of the helium core m_c at the end of the main sequence we use (Eggleton, private communication, 1998)

$$m_c = \frac{0.11\ M^{1.2} + 7\ 10^{-5}\ M^4}{1 + 2\ 10^{-4}\ M^3}. \quad (A.1)$$

The mass of the core during the further evolution of the star is computed by integrating the growth of the core resulting from hydrogen shell burning:

$$\dot{m_c} = \eta_H \frac{L}{X} \quad (A.2)$$

where

$$\eta_H = 9.6\ 10^{-12}\ M_\odot\ \mathrm{yr}^{-1}\ L_\odot^{-1} \quad (A.3)$$

and X is the mass fraction of hydrogen in the envelope. During core helium burning we assume that half of the luminosity of the star is produced by hydrogen shell burning, while in the double shell burning phase we assume that all of the luminosity is produced by the hydrogen shell burning.

When giants have degenerate cores, application of a core mass–luminosity relation gives more accurate results than direct integration of the growth of the core.

For degenerate helium cores of stars with $M \lesssim 2.3\ M_\odot$ we use (Boothroyd & Sackmann 1988)

$$M_c = 0.146\ L^{0.143} \quad (A.4)$$

(all quantities in solar units). For degenerate CO cores of stars with $M \lesssim 8\ M_\odot$ on the AGB we use (Groenewegen & de Jong 1993)

$$\begin{aligned} M_c &= 0.015 + \sqrt{\frac{L}{47\,488} + 0.1804} && L < 15\,725 \\ M_c &= 0.46 + \frac{L}{46\,818}\ M^{-0.25} && L > 15\,725 \end{aligned} \quad (A.5)$$

where the transition between the two fits occurs at $M_c \approx 0.73\ M_\odot$ in stars $\sim$3.5 $M_\odot$ where the two relations fit together reasonably. We changed the power of the dependence on M from -0.19 in the original paper to -0.25 because the maximum luminosities given by our fits otherwise lead to white dwarf masses too high compared to initial–final mass relations as found from observations (see Groenewegen & de Jong 1993).

The masses of CO cores formed by central He burning inside the helium core are defined in the same way as we define the relation between the mass of helium stars and their CO cores (see Sect. A.1.2).

A white dwarf forms if a component of a binary with $M < 10\ M_\odot$ loses its hydrogen envelope through RLOF either before core helium burning (case B mass transfer) or after helium exhaustion (case C). The masses of white dwarfs formed in cases B and C as function of initial mass are shown in Fig. A.1.

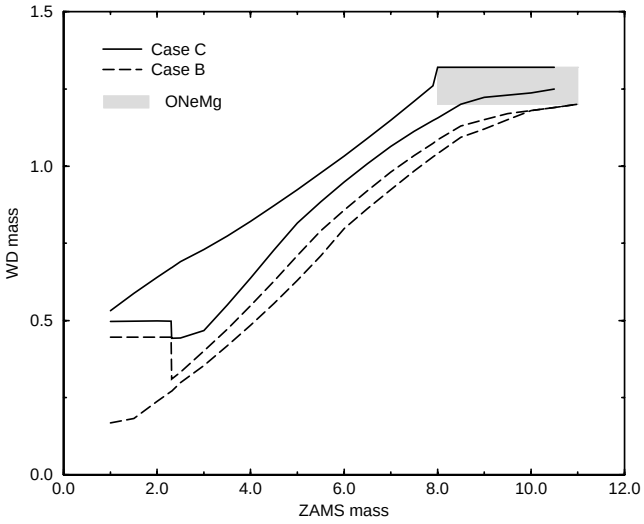

Fig. A.1. White dwarf masses as function of the ZAMS mass. Dashed lines are for case B mass transfer. The white dwarfs that descend from stars with ZAMS masses below 2.3 $M_\odot$ in case B mass transfer are helium white dwarfs. The two dashed lines give the minimum and maximum mass of the white dwarf, which depends on the orbital separation at the onset of the mass transfer. Solid lines are for case C mass transfer, which results in the formation of a CO white dwarf. When the ZAMS mass is above 8 $M_\odot$ the stripping of the envelope in case C mass transfer may prevent the formation of a neutron star, leading to the formation of a white dwarfs with a core consisting of O, Ne and Mg (shaded region)

A.1.2. Helium stars

A helium star is formed when a star more massive than 2.3 $M_\odot$ loses its hydrogen envelope in case B mass transfer. The helium star starts core helium burning and forms a CO core. In our code, this core grows linearly at a rate given by the ratio of 65% of the initial mass of the helium star and the total lifetime of the helium star. This is suggested by computations of Habets (1986) and gives a CO core of the Chandrasekhar mass for a 2.2 $M_\odot$ helium star; the minimum mass to form a neutron star in our code.

Helium stars with $0.8 \lesssim M \lesssim 3\ M_\odot$ expand again after core helium exhaustion and can lose their remaining helium envelope in so called case BB mass transfer. The amount of mass that can be lost is defined as increasing linearly from 0 to 45% for stars between 0.8 and 2.2 $M_\odot$ and stays constant above 2.2 $M_\odot$. The maximum mass of the CO white dwarf thus formed is 1.21 $M_\odot$. Helium stars of lower mass ($M < 0.8\ M_\odot$) do not expand and retain their thick helium envelopes, forming hybrid white dwarfs (Iben & Tutukov 1985).

Table A.1. Gyration radii for various types of stars

Type	k^2
Radiative stars	0.03
Convective stars	0.2
White dwarfs	0.4
Neutron stars	0.25[a]
Black holes	$\frac{1}{c\,R^2}$

(a) Gunn & Ostriker (1969).

A.1.3. Stellar wind

We describe mass loss in a stellar wind in a very general way in which the amount of wind loss increases in time according to

$$\Delta M_{\rm w} = M_{\rm lost}\,\left[\left(\frac{t+\Delta t}{t_{\rm f}}\right)^{\eta} - \left(\frac{t}{t_{\rm f}}\right)^{\eta}\right]. \qquad \text{(A.6)}$$

The exponent $\eta = 6.8$ is derived from fitting stellar wind mass loss on the main sequence of massive stars ($M \gtrsim 15\ M_\odot$ Meynet et al. 1994), but we apply it also for low and intermediate mass stars. For these stars $t_{\rm f}$ is the duration of the evolutionary phase that the star is in (as given by Eggleton et al. 1989). For the different evolutionary phases, the parameters $M_{\rm lost}$ is defined as follows.

In the Hertzsprung gap $M_{\rm lost}$ is 1% of the total mass of the star.

For the first giant branch (hydrogen shell burning), we use a fit to models of Sweigart et al. (1990) for stars with degenerate helium cores

$$M_{\rm lost} = (2.5 - M)/7.5\ M_\odot \qquad \text{(A.7)}$$

which we extend to all low and intermediate mass stars by setting $M_{\rm lost} = 0$ above $M = 2.5\ M_\odot$.

On the horizontal branch $M_{\rm lost}$ is 5% of the envelope mass.

For the AGB phase we take $M_{\rm lost}$ equal to 80% of the mass of the envelope of the star when it enters the early AGB phase.

A.1.4. Radii of gyration

In the previous version of the SeBa code all gyration radii were set to 0.4. The gyration radius plays a role in the determination of the stability of the mass transfer (Portegies Zwart & Verbunt 1996, Appendix C.1). We now use the following values.

For main-sequence stars we use a fit to the results by Claret & Giménez (1990). Further we classify stars either as radiative (stars in Hertzsprung gap and helium stars) or as convective (red giants, AGB stars). A summary of radii of gyration are given in Table A.1.

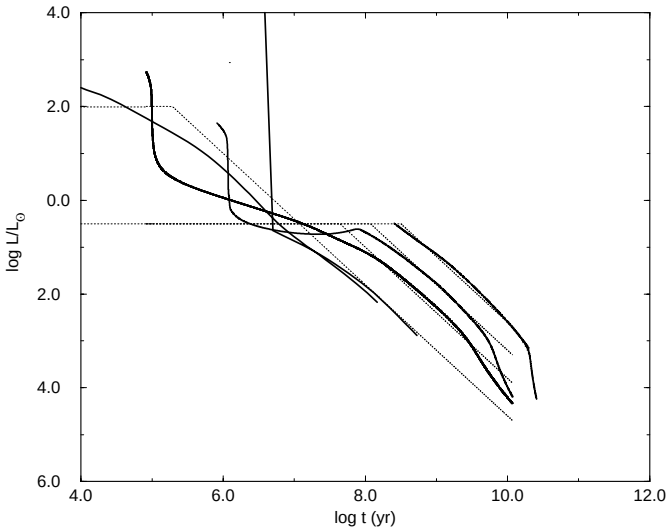

Fig. A.2. White dwarf cooling tracks from Driebe et al. (1998) and Blöcker (1995). Straight lines are the fits to these curves. The curves are for masses of 0.179, 0.300, 0.414, 0.6 and 0.8 from top right to bottom left

A.1.5. White dwarf evolution: Luminosity and radius

We model the cooling of white dwarfs according to the results of Blöcker (1995) and Driebe et al. (1998).

Luminosity
The luminosity of white dwarfs as function of time t can be reasonably well modelled by

$$\log L = L_{\rm max} - 1.4\log(t/10^6\ {\rm yr}) \qquad \text{(A.8)}$$

where $L_{\rm max}$ is a linear fit given by

$$L_{\rm max} = 3.83 - 4.77\ M_{\rm WD} \quad \text{for } 0.18 < M_{\rm WD} < 0.6 \qquad \text{(A.9)}$$

(mass and luminosity in solar units). Outside these limits $L_{\rm max}$ stays constant (i.e. $L_{\rm max} = 3$ below $M_{\rm WD} = 0.18$ and $L_{\rm max} = 1$ above $M_{\rm WD} = 0.6$). For white dwarf masses below 0.6 $M_\odot$ the luminosity is constrained to be below $\log L/L_\odot = -0.5$, for more massive white dwarfs below $\log L/L_\odot = 2$. In Fig. A.2 we show the fits and the results of Blöcker (1995) and Driebe et al. (1998).

Radius
We fitted the models of Driebe et al. (1998) and Blöcker (1995), and interpolated between the fits. The fits are given by

$$\frac{R}{R_\odot} = a - b\log(t/10^6\ {\rm yr}) \quad \text{for } M_{\rm WD} < 0.6\ M_\odot. \qquad \text{(A.10)}$$

The coefficients a and b are given in Table A.2. Figure A.3 shows the fits and the corresponding detailed calculations.

For more massive white dwarfs we use the mass-radius relation for zero-temperature spheres (Nauenberg 1972)

$$\frac{R}{R_\odot} = 0.01125\,\sqrt{\left(\frac{M_{\rm WD}}{M_{\rm Ch}}\right)^{-2/3} - \left(\frac{M_{\rm WD}}{M_{\rm Ch}}\right)^{2/3}}. \qquad \text{(A.11)}$$

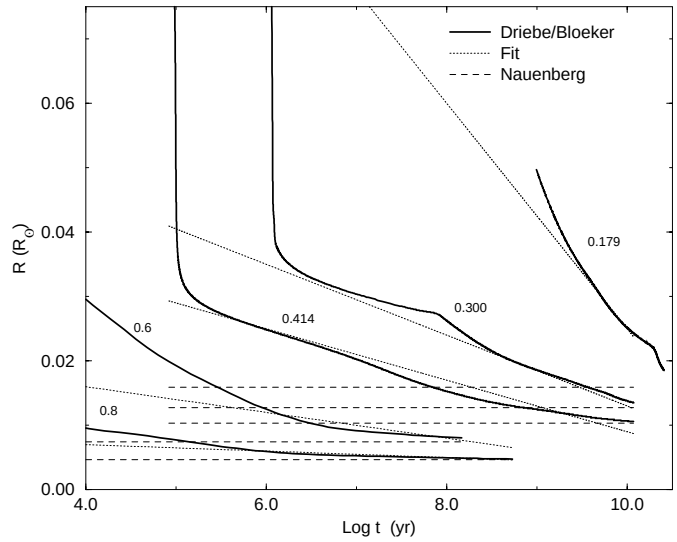

Fig. A.3. White dwarf radii from Driebe et al. (1998) and Blöcker (1995). Straight lines are the fits to these curves. The curves are for masses of 0.179, 0.300, 0.414, 0.6 and 0.8 from top right to bottom left

A.1.6. Modified DSBH98 cooling

Our modification to the cooling described above reduces the cooling time scale for white dwarfs with masses below 0.3 $M_\odot$. For these white dwarfs we use the cooling curve and the radius of a more massive, thus faster cooling white dwarf of 0.46 $M_\odot$ (see Sect. 4.3).

A.2. Mass transfer in binary stars

As suggested by Nelemans et al. (2000), we distinguish four types of mass transfer with different outcomes: stable mass transfer, common envelope evolution, envelope ejection and a double spiral-in.

A.2.1. Stable mass transfer

The amount of mass that can be accreted by a star is limited by its thermal time scale

$$\dot{M}_{\rm max} \approx \frac{M}{\tau_{\rm th}} \approx \frac{R\,L}{G\,M}. \qquad \text{(A.12)}$$

If not all mass can be accreted, we assume that the excess of mass leaves the system taking with it $n_{\rm J}$ times the specific angular momentum of the binary.

This assumption gives for the variation of orbital separation

$$\frac{a_{\rm f}}{a_{\rm i}} = \left(\frac{M_{\rm f}\,m_{\rm f}}{M_{\rm i}\,m_{\rm i}}\right)^{-2} \left(\frac{M_{\rm f}+m_{\rm f}}{M_{\rm i}+m_{\rm i}}\right)^{2n_{\rm J}+1}. \qquad \text{(A.13)}$$

We use $n_{\rm J} = 2.5$, which gives good agreement for the periods of low-mass Algols and Be X-ray binaries (Portegies Zwart 1996).

Table A.2. Coefficients for the fits to the white dwarf radii

$M_{\rm WD}$	a	b
0.2	0.1	0.0175
0.4	0.03	0.0044
0.6	0.017	0.001
0.8	0.011	0.0005

A.2.2. Standard common envelope

When the mass transfer is unstable due to a tidal instability, the accretor is a compact object, or the envelope ejection equation gives a smaller orbital separation, we apply the standard common envelope equation $E_{\rm bind} = \alpha_{\rm ce}\,\Delta E_{\rm orb}$ (Webbink 1984):

$$\frac{M_{\rm i}\,(M_{\rm i}-M_{\rm f})}{\lambda\,R} = \alpha_{\rm ce}\,\left[\frac{M_{\rm f}\,m}{2\,a_{\rm f}} - \frac{M_{\rm i}\,m}{2\,a_{\rm i}}\right] \qquad \text{(A.14)}$$

where $\alpha_{\rm ce}$ is an efficiency parameter and λ a parameter describing the strucure of the envelope of the giant. Both are uncertain so we use them combined: $\alpha_{\rm ce}\,\lambda = 2$.

A.2.3. Envelope ejection

In the case of envelope ejection (Nelemans et al. 2000), we assume that the complete envelope is lost and that this mass loss reduces the angular momentum of the system linearly proportional to the mass loss, as first suggested for the general case of non-conservative mass transfer by Paczyński & Ziołkowski (1967)

$$J_{\rm i} - J_{\rm f} = \gamma J_{\rm i} \frac{\Delta M}{M_{\rm tot}}, \qquad \text{(A.15)}$$

where $J_{\rm i}$ is the angular momentum of the pre-mass transfer binary and $M_{\rm tot}$ is the total mass of the binary. The companion does not accrete al all (see discussion in Sect. 2.2 and Nelemans et al. 2000). The change in orbital separation is given by

$$\frac{a_{\rm f}}{a_{\rm i}} = \left(\frac{M_{\rm f}\,m_{\rm f}}{M_{\rm i}\,m_{\rm i}}\right)^{-2} \left(\frac{M_{\rm f}+m_{\rm f}}{M_{\rm i}+m_{\rm i}}\right) \left(1-\gamma\frac{M_{\rm i}-M_{\rm f}}{M_{\rm i}+m_{\rm i}}\right)^{2}. \qquad \text{(A.16)}$$

In this work we use $\gamma = 1.75$.

A.2.4. Double spiral-in

If mass transfer is unstable when both stars are evolved (which can only happen if the mass ratio is close to unity), we model the evolution as a common envelope in which the two cores spiral-in. The energy needed to expel the complete envelope is computed analogously to the case of a standard common envelope (Webbink 1984; see also Sect. A.2.2):

$$\frac{M_{\rm i}\,(M_i-M_{\rm f})}{\lambda\,R} + \frac{m_{\rm i}\,(m_{\rm i}-m_{\rm f})}{\lambda r} = \alpha_{\rm ce}\,\left[\frac{M_{\rm f}\,m_{\rm f}}{2\,a_{\rm f}} - \frac{M_{\rm i}\,m_{\rm i}}{2\,a_{\rm i}}\right].$$

If the final separation is too small for the two cores to form a detached binary, the cores merge and we compute the

fraction of the envelopes that is lost with the (practical) assumption that both stars lose the same fraction of mass, retaining fM, i.e.

$$\frac{M_{\rm i}(1-f)M_{\rm i}}{\lambda\, R} + \frac{m_{\rm i}(1-f)m_{\rm i}}{\lambda r} = \alpha_{\rm ce}\left[\frac{fM_{\rm i}\, fm_{\rm i}}{2\, a_{\rm RLOF}} - \frac{M_{\rm i}\, m_{\rm i}}{2\, a_{\rm i}}\right]$$

where $a_{\rm RLOF}$ is the separation at which one of the cores fills its Roche lobe. This is solved for f.

References

Abt, H. A. 1983, ARA&A, 21, 343
Bergeron, P., Saffer, R. A., & Liebert, J. 1992, ApJ, 394, 228
Bergeron, P., Ruiz, M. T., & Leggett, S. K. 1997, ApJS, 108, 339
Blöcker, T. 1995, A&A, 299, 755
Boothroyd, A. I., & Sackmann, I. J. 1988, ApJ, 328, 641
Bragaglia, A., Renzini, A., & Bergeron, P. 1995, ApJ, 443, 735
Brown, G. E. 1995, ApJ, 440, 270
Cappellaro, E., Evans, R., & Turatto, M. 1999, A&A, 351, 459
Claret, A., & Giménez, A. 1990, Ap&SS, 169, 215
De Kool, M., van den Heuvel, E. P. J., & Pylyser, E. 1987, A&A, 183, 47
Driebe, T., Schönberner, D., Blöcker, T., & Herwig, F. 1998, A&A, 339, 123 (DSBH98)
Driebe, T., Blöcker, T., Schönberner, D., & Herwig, F. 1999, A&A, 350, 89
Duquennoy, A., & Mayor, M. 1991, A&A, 248, 485
Eggleton, P. P., Fitchett, M. J., & Tout, C. A. 1989, ApJ, 347, 998
Evans, C. R., Iben, I. Jr, & Smarr, L. 1987, ApJ, 323, 129
Festin, L. 1998, A&A, 336, 883
Giannone, P., & Giannuzzi, M. A. 1970, A&A, 6, 309
Groenewegen, M. A. T., & de Jong, T. 1993, A&A, 267, 410
Gunn, J. E., & Ostriker, J. P. 1969, Nat, 221, 454
Habets, H. J. 1986, A&A, 167, 61
Han, Z. 1998, MNRAS, 296, 1019 (HAN98)
Han, Z., Podsiadlowski, P., & Eggleton, P. P. 1995, MNRAS, 272, 800
Hansen, B. M. S. 1999, ApJ, 520, 680
Hils, D., Bender, P. L., & Webbink, R. F. 1990, ApJ, 360, 75
Iben, I. Jr, & Livio, M. 1993, PASP, 105, 1373
Iben, I. Jr, & Tutukov, A. V. 1984, ApJS, 54, 355
Iben, I. Jr, & Tutukov, A. V. 1985, ApJS, 58, 661
Iben, I. Jr, & Tutukov, A. V. 1986a, ApJ, 311, 753
Iben, I. Jr, & Tutukov, A. V. 1986b, ApJ, 311, 742
Iben, I. Jr, & Tutukov, A. V. 1987, ApJ, 313, 727
Iben, I. Jr, Tutukov, A. V., & Yungelson, L. R. 1997, ApJ, 475, 291 (ITY97)
Iben, I. Jr, Tutukov, A. V., & Fedorova, A. V. 1998, ApJ, 503, 344
Kippenhahn, R., Thomas, H. C., & Weigert, A. 1968, ZsAp, 69, 265
Knox, R., Hawkins, M. R. S., & Hambly, N. C. 1999, MNRAS, 306, 736
Koen, C., Orosz, J. A., & Wade, R. A. 1998, MNRAS, 300, 695
Lipunov, V. M., & Postnov, K. A. 1988, Ap&SS, 145, 1
Livio, M. 1999, in Type Ia Supernovae: Theory and Cosmology, ed. J. A. Truran, & J. Niemeyer (CUP, Cambridge), [astro-ph/9903264]
Marsh, T. R. 2000, NewAR, 44, 119
Marsh, T. R., Dhillon, V. S., & Duck, S. R. 1995, MNRAS, 275, 828
Maxted, P. F. L., & Marsh, T. R. 1999, MNRAS, 307, 122
Maxted, P. F. L., Marsh, T. R., Moran, C. K. J., & Han, Z. 2000, MNRAS, 314, 334
Maxted, P. F. L., Marsh, T. R., & North, R. C. 2000, MNRAS, 317, L41
Meynet, G., Maeder, A., Schaller, G., Schaerer, D., & Charbonnel, C. 1994, A&AS, 103, 97
Miller, G. E., & Scalo, J. M. 1979, ApJS, 41, 513
Moran, C., Maxted, P. F. L., & Marsh, T. R. 1999, MNRAS, 304, 535
Moran, C. K. J., Maxted, P. F. L., & Marsh, T. R. 2000, MNRAS, submitted
Napiwotzki, R., Green, P. J., & Saffer, R. A. 1999, ApJ, 517, 399
Nauenberg, M. 1972, ApJ, 417
Nelemans, G., Portegies Zwart, S. F., Verbunt, F., & Yungelson, L. R. 2001, A&A, submitted
Nelemans, G., Verbunt, F., Yungelson, L. R., & Portegies Zwart, S. F. 2000, A&A, 360, 1011
Orosz, J. A., & Wade, R. A. 1999, MNRAS, 310, 773
Oswalt, T., Smith, J., Wood, M. A., & Hintzen, P. 1995, Nat, 382, 692
Paczyński, B. 1976, in Structure and Evolution of Close Binary Systems, ed. P. Eggleton, S. Mitton, & J. Whelan (Kluwer, Dordrecht), 75
Paczyński, B., & Ziołkowski, J. 1967, Acta Astron., 17, 7
Portegies Zwart, S. F. 1996, A&A, 296, 691
Portegies Zwart, S. F., & Verbunt, F. 1996, A&A, 309, 179
Portegies Zwart, S. F., & Yungelson, L. R. 1998, A&A, 332, 173
Pottasch, S. R. 1996, A&A, 307, 561
Rana, N. C. 1991, ARA&A, 29, 129
Refsdal, S., & Weigert, A. 1970, A&A, 6, 426
Ruiz, M. T., & Takamiya, M. 1995, AJ, 109, 2817
Sackett, P. D. 1997, ApJ, 483, 103
Saffer, R. A., Liebert, J., & Olszewski, E. W. 1988, ApJ, 334, 947
Saffer, R. A., Livio, M., & Yungelson, L. R. 1998, ApJ, 502, 394
Sandquist, E. L., Taam, R. E., & Burkert, A. 2000, ApJ, 533, 984
Sarna, M., Ergma, E., & Gerskevits-Antipova, J. 2000, MNRAS, 316, 84
Sweigart, A. V., Greggio, L., & Renzini, A. 1990, ApJ, 364, 527
Tout, C. A., & Eggleton, P. P. 1988, MNRAS, 231, 823
Tout, C. A., Aarseth, S. J., Pols, O. R., & Eggleton, P. P. 1997, MNRAS, 291, 732
Tutukov, A. V., & Yungelson, L. R., 1979, in Mass loss and evolution of O-type stars, ed. C. de Loore, & P. S. Conti (Reidel, Dordrecht) 401
Tutukov, A. V., & Yungelson, L. R. 1993, SvA, 36, 266
Tutukov, A. V., & Yungelson, L. R. 1994, MNRAS, 268, 871
Tutukov, A. V., & Yungelson, L. R. 1996, MNRAS, 280, 1035
van den Hoek, L. B., & de Jong, T. 1997, A&A, 318, 231
van Kerkwijk, M. H., Bell, J. F., Kaspi, V. M., & Kulkarni, S. R. 2000, ApJ, 530, 37
Webbink, R. F. 1975, MNRAS, 171, 555
Webbink, R. F. 1984, ApJ, 277, 355
Yungelson, L. R., Livio, M., Tutukov, A. V., & Saffer, R. 1994, ApJ, 420, 336